Available online at www.sciencedirect.com
ScienceDirect
Bioorganic & Medicinal Chemistry Letters 16 (2006) 6013–6018
Bioorganic & Medicinal Chemistry Letters

Comparative protein modeling and surface analysis of Leishmania sirtuin: A potential target for antileishmanial drug discovery

Rameshwar U. Kadam, Kiran V. M. and Nilanjan Roy*

Centre of Pharmacoinformatics, National Institute of Pharmaceutical Education and Research, Sector 67, S. A. S. Nagar, Punjab 160062, India

Received 8 June 2006; revised 8 August 2006; accepted 30 August 2006
Available online 18 September 2006

Abstract—Homology model of *Leishmania* SIR2 shed new light on the ligand binding features of this enzyme. The molecular electrostatic potentials (MESP), the cavity depth analysis, and LmSIR2–hSIRT2 models' superposition suggested that the nicotinamide binding catalytic domain has several minor but potentially important structural differences. These differences could be exploited for designing antileishmanial compounds.

Leishmaniasis is a complex disease caused by at least 17 different species of the protozoan parasite *Leishmania*. The parasite exists in two forms; the flagellated promastigote in the female phlebotomine sandfly vector and the amastigote in the mammalian host. Amastigotes are obligate intracellular parasites of macrophages (and rarely other cell types), where they survive and multiply within a phagolysosome compartment. Leishmaniasis has traditionally been classified in three different clinical forms, visceral leishmaniasis (VL), cutaneous leishmaniasis (CL), and mucocutaneous leishmaniasis (MCL), which have different immunopathologies and degrees of morbidity and mortality. VL caused by *Leishmania donovani* is fatal if untreated, whereas CL, caused by species such as *Leishmania major*, *Leishmania mexicana*, *Leishmania braziliensis*, and *Leishmania panamensis*, frequently selfcures within 3–18 months, leaving disfiguring scars. Although human leishmaniasis is distributed worldwide, it is more frequent in the tropics and sub-tropics, with a prevalence of over 12 million cases and an approximated incidence of 0.5 and 1.5 million cases of VL and CL, respectively. General aspects of leishmaniasis and overall control strategies have been reviewed recently.[1,2] In the recent years, visceral leishmaniasis is reported to be rapidly emerging as an opportunistic infection in HIV patients,[3,4] in pregnant females, and in organ transplant patients.[5,6] Globalization and consequent travel of people across the world has increased the chances of spreading the infection.[7,8]

Pentavalent antimonials were brought into use against this disease more than 50 years ago. Along with pentamidines, polyene antibiotic amphotericin B have also proved to be successful for the treatment of *L. donovani* VL. However, these have the disadvantage of high toxicity. Immunocompromised leishmaniasis patients, especially those co-infected with HIV, are difficult to treat with conventional drugs because relapses can occur and repeated treatment is required.

Since the available treatment for leishmaniasis poses many problems, researchers are looking at novel biochemical targets in order to develop new drugs. In 1996, Ouaissi group had cloned a *L. major* SIR2 gene (LmSIR2) encoding a protein, bearing characteristics of sirtuin proteins.[9] Overexpression of LmSIR2 increased the survival of amastigotes[10] and sirtinol, a sirtuin inhibitor, showed a stage specific cell killing activity against *Leishmania* parasites *in vivo*[11] while nicotinamide inhibits LmSIR2 in vitro.[12] Results depicted in the literature demonstrate that LmSIR2 protects parasites against environmental stress and may be considered as a potential drug target. Since, SIR2 is present in human as well; the inhibitor for the purpose of drug design needs to have selectivity for the parasite target. This study was performed with the aim to understand the active site and the binding

Abbreviations: NAM, nicotinamide; NAC, nicotinic acid; SIR2, silent information regulator2; MOE, molecular operating environment.
Keywords: Leishmania; Sir2 NAD; Homology modeling; MOE; MEPS.
* Corresponding author. Tel.: +91 172 2214 682 87x2067; fax: +91 172 2214 692; e-mail: nilanjanroy@niper.ac.in

0960-894X/$ - see front matter © 2006 Published by Elsevier Ltd.
doi:10.1016/j.bmcl.2006.08.128

characteristics of the ligands in the target. Molecular electrostatic potential surface analysis and cavity depth analysis of both the proteins revealed characteristic differences between LmSIR2 and hSIRT2 which can be exploited for selective ligand design.

All computations and molecular modeling of LmSIR2 were carried out on a Silicon Graphics Fuel Work station with IRIX 6.5 operating system using the MOE-03 (Molecular Operating Environment)[13] and SYBYL6.9[14] molecular modeling packages. Homology modeling module of the MOE was used for comparative protein modeling. The amino acid sequence of *Leishmania* SIR2 was obtained from the NCBI protein database (SIR2_LEIMA; SWISSPROT Accession No. Q25337) and WU-BLAST (Washington University BLAST)[15] retrieved four sirtuin crystal structures from Protein Data Bank[16] (Table 1).

Sequence alignment was done using 'Roundrobin iterative refinement option' and 'tree based alignment approach' in MOE-Align module. BLOSUM62 matrix was used and all the templates were aligned against SIR2_LEIMA sequence. Manual alignment was done at certain regions.

Homology modeling module of MOE was used for the model building. Employing Coarse model refinement 10 independent models were constructed by the Boltzmann-weighted randomized modeling procedure. Each of these intermediate models was subjected to a sufficient degree of minimization to relieve any serious steric clashes. The model with the best packing quality was chosen and subjected to minimization steps. Validation of the model was done with PROCHECK.[17] Subsequently, homology model of LmSIR2 was superimposed onto the hSIRT2 crystal structure (1J8F) and corresponding residues within a radius of 7 Å of the substrate (NAD) binding in the 1J8F crystal structure were identified.

The electrostatic interaction is a crucial part of the noncovalent interaction energy between molecules. The electrostatic potential on a molecular surface can be used to visually compare two molecules, guiding docking studies and identifying sites that interact with ligands because of opposite electrostatics. The following equation is used to calculate the MEP values.

$$\mathrm{EP}(i) = \sum_{j=1}^{N} \frac{q_i}{r_{ij}} \quad (1)$$

where $\mathrm{EP}(i)$ is the electrostatic potential at the surface point i due to atom j having the partial charge q_j and separated by distance r_{ij}. The electrostatic potential (EP) on the surface is generally colored according to the sign and magnitude of the potential. The color ramp for EP ranges from red (most positive) to purple (most negative). To understand more characteristic differences in active site of LmSIR2 and hSIRT2, we performed cavity depth analysis along with MEP calculation.

The cavity depth measures how deep a surface point is located inside a cavity of a molecule. The calculation of this property is based on the difference of two molecular surfaces. The unit of the cavity depth is Å. The color ramp for cavity depth ranges from blue color (low depth value) to light red (high depth value).

All MEP and cavity depth analysis calculations and visualization were carried out using the MOLCAD program implemented in the SYBYL6.9 molecular modeling package. The Gasteiger-Hückel charges were assigned to the atoms of both structures (LmSIR2 and hSIRT2) and surfaces were generated and visualized.

Strategy used for homology modeling of the LmSIR2 is described below. WU-Blast2 server (Washington University Basic Local Alignment Search Tool; http://www.ebi.ac.uk/blast2/) and BLOSUM 62 matrix with an *E*-value cut off of 10 were used for the template search. The results revealed the presence of four sirtuin crystal structures, which could be used as template for LmSIR2 modeling (Table 1). The best hit, human SIRT2 (1J8F), was aligned pairwise (globally) with LmSIR2 using Needleman–Wunsch Dynamic programming to identify the overall similarity between the protein sequences (needle program in EMBOSS).[18] The identity and similarity between the target and template was 33.5% and 49.6%, respectively. Since the two proteins presented good alignment in the N-terminal region, 250 amino acid sequences in N-termini of both the proteins were taken for local alignment using water algorithm in EMBOSS package. This alignment showed 45.7% identity and 65.8% similarity between the sequences indicating high conservation along the N-termini of the two proteins. This region includes the substrate-binding site of the enzyme.

The four crystal structures from WU-BLAST search were used to provide overlapping structural data for the model building. Structure based information was incorporated to the process for final multiple-sequence alignment (Fig. 1) which showed regions corresponding to residues R270 to E287 and A304 to D328 in LmSIR2 sequence as difficult to model regions. These regions did not have any structural coordinate information from any templates from PDB. The consensus secondary structure prediction programs in Expasy predicted the regions to be predominantly random coils. This indicated that modeling of these regions could be difficult and

Table 1. Selected templates for modeling, showing percentage identity with LmSIR2 using MOE-align, along with PDB CODE and resolution in (Å) unit

Name	Source	Identity with LmSIR2 (%)	PDB code	Resolution (Å)
SIRT2	*Homo sapiens*	42	1J8F	1.700
yHST2	*Saccharomyces cerevisiae*	36	1Q14	2.500
Sir2Af2	*Archaeoglobus fulgidus*	32	1ICI	2.100
Sir2	*Escherichia coli*	30	1S5P	1.960

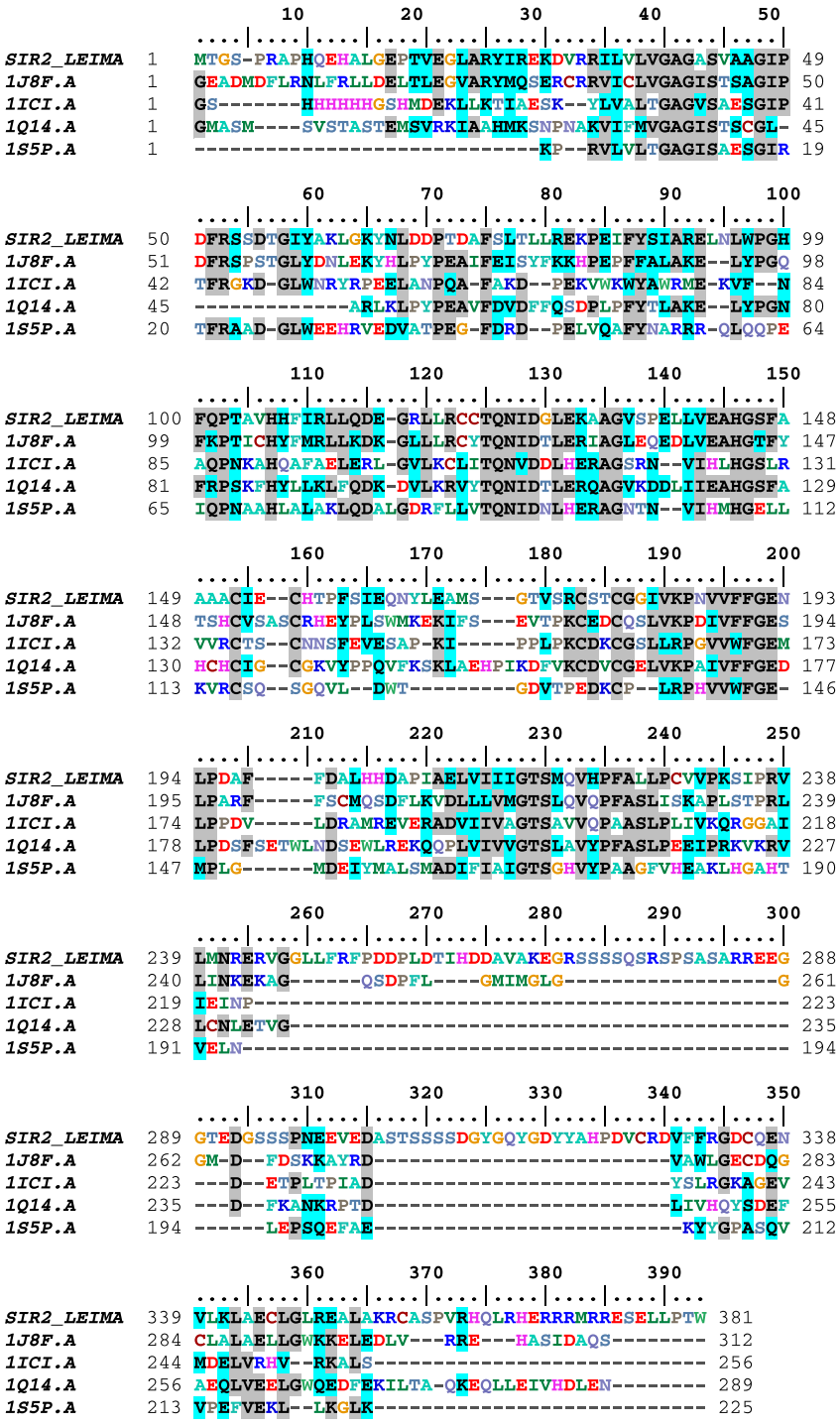

Figure 1. Multiple-sequence alignment of *Leishmania* SIR2 with the templates (SIRT2, yHST2, Sir2Af2, and Sir2). Gray areas indicate the highly conserved regions in sirtuin family.

may be unreliable. BLASTP against non-redundant protein database in NCBI showed these regions have similarity only to *Trypanosoma brucei* Sir2 homologue (EMBL: O96670) (similarity 63%) apart from similarity to homologues in other *Leishmania* species. This indicates that these regions may be characteristic of these closely related species. Manual alignment was done at region where the cysteine disulfide bridge was present which corresponds to region C152 to C193 of LmSir2 (Fig. 1). Since default alignment did not align this region properly cysteine residues were aligned manually.

Accordingly, structurally conserved regions (SCR) and structurally variable regions (SVR) were defined, and the model was built using human SIRT2 as the primary template. The best of the 10 models built with good packing quality was chosen as the final model. To control the degree of refinement by molecular mechanics

to apply to the final model, the model was subjected to a highly tethered series of conjugate gradient minimization steps. The medium minimization options using Truncated Newton optimization algorithm, with RMS gradient tests of 1 Å, were employed.

The quality of the modeled structure was assessed using Ramachandran plot in PROCHECK validation package. After refinement, 95.7% of the residues were in the allowed region, 2.7% were in the generously allowed region. This indicated that the backbone dihedral angles, phi and psi, in the model were reasonably accurate. The residues in the disallowed region accounted only for 1.6% of the total protein. As the four residues in this disallowed region were not a part of the active site under investigation (Fig. 2), attempts to further refine the model were not performed.

The LmSIR2 model exhibited the same overall folds of the sirtuin family consisting of a large domain, a small domain, and a long loop. The large domain of LmSIR2 contains parallel beta sheets forming a Rossmann fold that is characteristic of many NAD/NADP binding enzymes. The small domain forms the roof of the nicotinamide group binding site. The large and small domains do not make direct interactions, but, have fixed orientation to each other by virtue of interactions that are mediated by the extended connection loops. The region between the small and large domains forms a pronounced groove that runs roughly perpendicular to the long axis of the molecule (Fig. 3). Studies on Sir2 family members have revealed that hydrolysis of NAD to nicotinamide and ADP-ribose is tightly coupled to the deacetylation of acetyl-lysine. Moreover, it has been suggested that this coupled reaction generates a novel product, 1-*O*-acetyl-ADP ribose, in which the acetyl group from acetyl-lysine is transferred to the nicotinamide position of NAD.[19–24]

According to functionality of the active site regions, the location of the active site has been referred to as

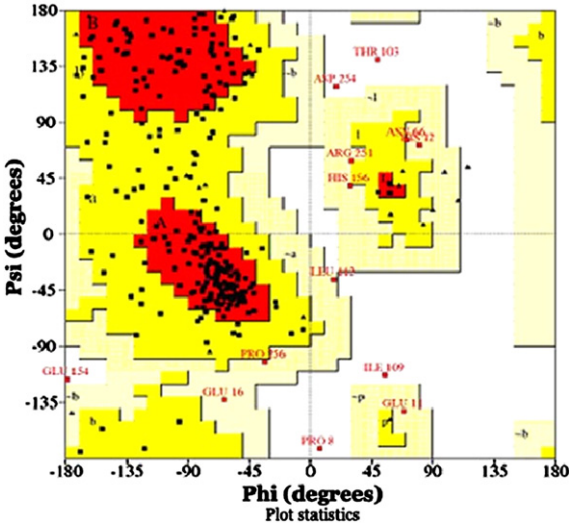

Figure 2. Ramachandran plot of LmSIR2 model by PROCHECK validation package.

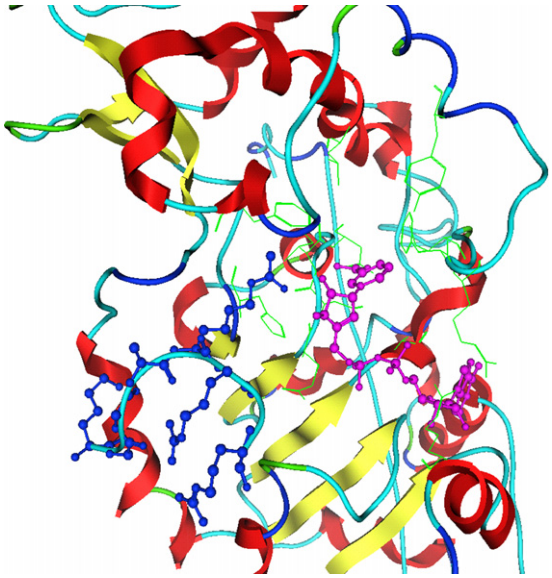

Figure 3. Structural topology of LmSIR2. Carton model represents overall folds of LmSIR2, NAD is colored magenta in a ball and stick model.

sites B and C.[19] Site B is located on the extreme edge of the conserved region close to the nicotinamide side of the NAD and contains an accessible and deep channel that possibly is the binding site for the substrate. This site has a chemical environment that is consistent with a putative role in acetyl-binding. Specifically, at the bottom of channel is a histidine residue, which is strictly conserved within the Sir2 family (His187 in

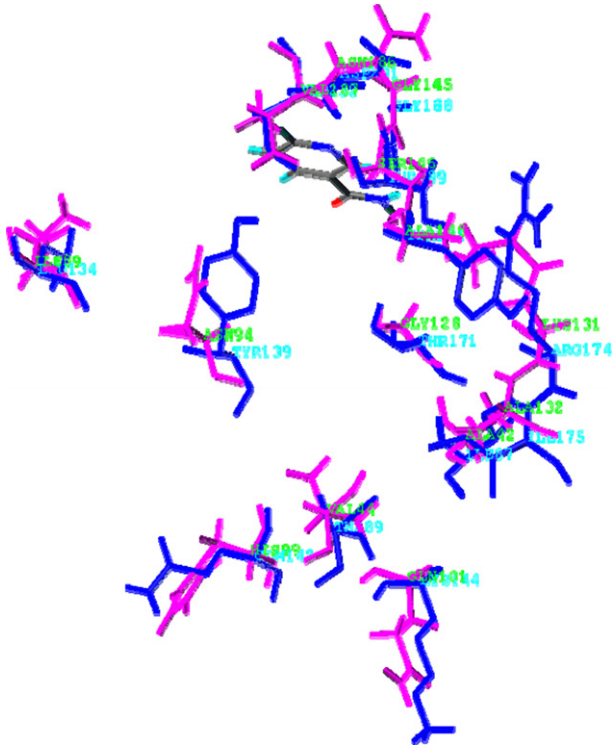

Figure 4. The active site residues of hSIRT2 (magenta) superposition onto the LmSIR2 (blue), along with ligand Nam interaction with active site.

hSIRT2) and is likely to play an important role in catalysis. In addition, the region close to the histidine residue and towards the outside of the channel contains conserved hydrophobic residues that may serve to complement the aliphatic chain acetyl-lysine. Subsequently, superposition of LmSIR2 and hSIRT2 reveals the characteristic differences in the active site (Fig. 4). The residues, Lys131, Ser146, Asn186, Val187, and Ala148 in LmSIR2 are replaced by Arg174, Thr189, Asp231, Ile232 and Tyr191 in hSIRT2, respectively. These relative differences in the active site should undoubtedly affect the steric and electrostatic interactions with inhibitors.

The MEP is a popular indicator of electrophilic and nucleophilic centers, which governs the strength of bonds, the strength of non-bonded interactions, and molecular reactivity. It affects the strength of the interaction of the ligand with the receptor protein. Bhattacharrjee and Karle have used the MEP to relate the antimalarial potency of carbinolamine analogs[25] and neurotoxicity of artemisinin analogs.[26] In case of a ligand–protein interaction at the active site, the ligand experiences a unique environment in terms of electrostatic, steric, and hydrophobic properties. Variations in these properties in the active sites of different proteins can contribute to selective/specific or tighter binding of the ligand to enzyme proteins. Thus, a comparison of the MEPs of LmSIR2 and hSIRT2 is one step toward understanding selectivity in LmSIR2 inhibition.

The MEP surfaces depicted in Figure 5A and B are shown with absolute values of the electrostatic potential for LmSIR2 (−7688 to −15,569 kcal/mol Å; Fig. 5A) and hSIRT2 (−7892 to −14,833 kcal/mol Å; Fig. 5B). Since the range of potentials in the two proteins is varying, electrostatic potential of the two proteins was placed on the same scale (−7688 to −15,569 kcal/mol Å; Fig. 5C) to make the comparison easier. As is evident in Fig. 5C, the electrostatic potential covering the active site residues in the two proteins has sharply differing values. Within the LmSIR2 active site, the surface around Phe147, Asp127, Gly128, and Asn125 residues has a relatively more electronegative potential than that created by Ile169, Asp170, Thr171, and Ile175 residues within hSIRT2 active site. Moreover, a contrasting feature is also visible for the region encompassing residues Phe51 and Leu93 within the LmSIR2 active site which is less electropositive as compared to the corresponding residues, Pro140 and Phe96, within hSIRT2 active site. Further, the difference in the value of the potential at Asp127 in LmSIR2 (−15,569 kcal/mol ’Å) and Asp170 in hSIRT2 (−14,371 kcal/mol Å) might have a good impact on the variable binding of NAD^+ which is responsible for the catalytic activity in sirtuins.[19] This means that the two proteins will bind the co-substrate

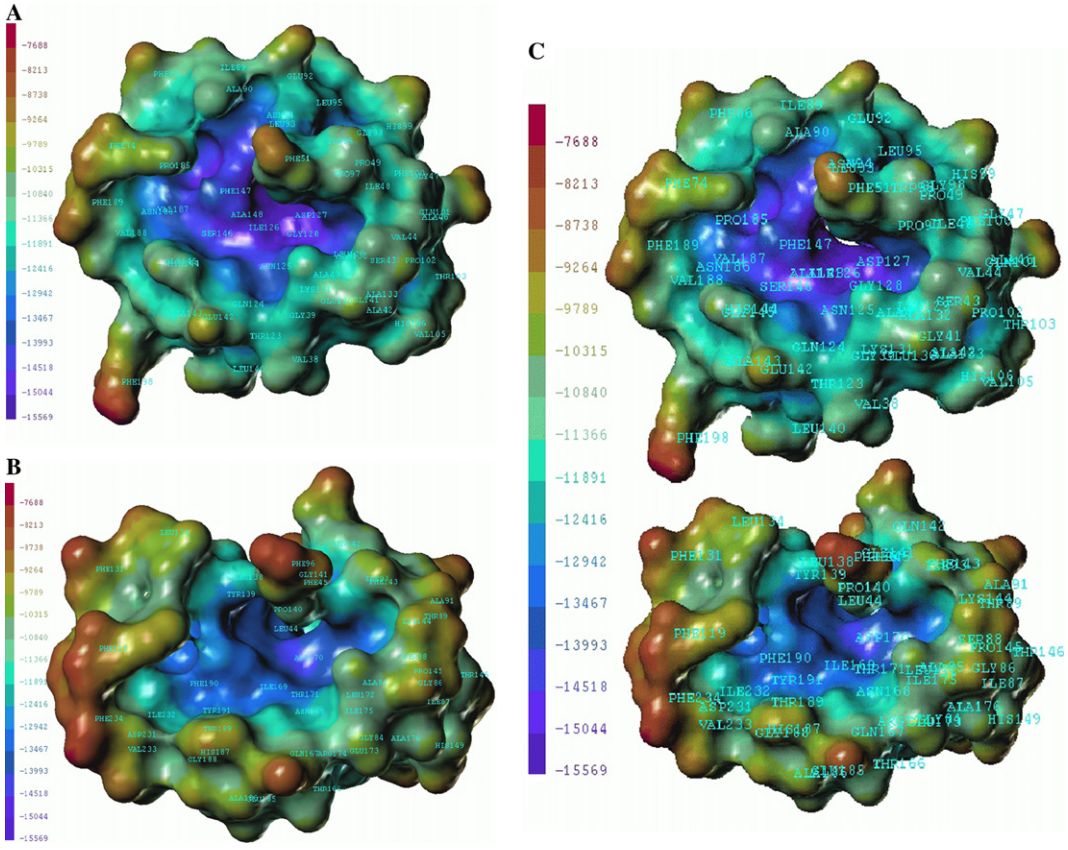

Figure 5. Absolute molecular electrostatic potential (MEP) values displayed for active sites of LmSIR2 (A) and h SIRT2 (B). The deep blue color indicates the highest negative potential, whereas the most positive potential is seen as a deep red color. The color spectrum shown to the left shows the gradation of electrostatic potential in the respective enzymes. In order to make valid comparisons between two models the electrostatic potentials have been put on the same scale (C).

(NAD^+) in the same relative sense, but with different binding affinities, due to the differences in the absolute values of the electrostatic potential.

Subsequent cavity depth analysis of both proteins revealed characteristic differences in the active site cleft near to B- and C-pocket. (Supplementary material-1; Fig. 1). In case of LmSIR2, area surrounding Ile126, Asp127, and Phe147 has depth value of 8.5 Å which is different from the corresponding Ile169, Asp170, Phe190 area in hmSIR2 which has a depth value of 6.7–7.3 Å. These differences in active sites of the two proteins can possibly make a reasonable contribution toward selective binding of substrates and affect the steric and electrostatic interactions of NAD^+ analogues if designed as inhibitors. Thus, along with MEPS and cavity depth analysis of LmSIR2 and hmSIR2 provides basic differences of active sites. However, molecular dynamics simulations on active site of both proteins may provide more clear and accurate understanding of active site and selective binding of substrates. These differences can possibly make a reasonable contribution toward selective binding of substrates.

The chemotherapy currently available for leishmaniasis is far from satisfactory and there is an urgent need for discovering and developing safe, inexpensive, and orally available drugs. The early stages of drug discovery are done in phases of target identification, validation, and hit/lead identification. In computer-aided drug design, knowledge of the three-dimensional structure of a protein is of immense importance. Predictions of tertiary structure can be made in the absence of crystallographic structures by the study of sequence–structure–function relationships. The most reliable method of protein structure prediction until now is modeling by homology. A 3D model of SIR2 in *L. major* was constructed by homology modeling technique. This resulted in reliable modeling of the ligand binding domain and shed new light on the binding features of this enzyme, which has not yet been crystallized. In particular, significant differences in the active sites for leishmania and human sirtuin were identified. The model suggested several minor but potentially important structural differences in the nicotinamide binding catalytic domain of the two proteins. These differences could be possibly exploited in future for design of antileishmanial compounds.

Supplementary data

Supplementary data associated with this article can be found, in the online version, at doi:10.1016/j.bmcl.2006.08.128.

References and notes

1. Guerina, P. J.; Olliarob, P.; Sundard, S.; Boelaerte, M.; Croftf, S. L.; Desjeuxg, P.; Wasunnah, M. K.; Bryceson, A. DM. *Lancet Infect. Dis.* **2002**, *2*, 494.
2. Davies, C. R.; Paul, K.; Croft, S. L.; Sundar, S. *BMJ* **2003**, *326*, 377.
3. Avalos, J. L.; Bever, K. M.; Wolberger, C. *Mol. Cell* **2005**, *17*, 855.
4. Berenguer, J.; Gomez-Campdera, F.; Padilla, B.; Rodriguez-Ferrero, M.; Anaya, F.; Moreno, S.; Valderrabano, F. *Transplantation* **1998**, *65*, 1401.
5. Berenguer, J.; Moreno, S.; Cercenado, E.; Bernaldo de Quiros, J. C.; Garcia de la Fuente, A.; Bouza, E. *Ann. Intern. Med.* **1989**, *111*, 129.
6. Berman, H. M.; Westbrook, J.; Feng, Z.; Gilliland, G.; Bhat, T. N.; Weissig, H.; Shindyalov, I. N.; Bourne, P. E. *Nucleic Acids Res.* **2000**, *28*, 235.
7. Lopez, R.; Silventoinen, V.; Robinson, S.; Kibria, A.; Gish, W. *Nucleic Acids Res.* **2003**, *31*, 3795.
8. Maguire, G. P.; Bastian, I.; Arianayagam, S.; Bryceson, A.; Currie, B. J. *Pathology* **1998**, *30*, 73.
9. Pagliano, P.; Carannante, N.; Rossi, M.; Gramiccia, M.; Gradoni, L.; Faella, F. S.; Gaeta, G. B. *J. Antimicrob. Chemother.* **2005**, *55*, 229.
10. Paredes, R.; Laguna, F.; Clotet, B. *J. Int. Assoc. Physicians AIDS Care* **1997**, *3*, 22.
11. Scope, A.; Trau, H.; Anders, G.; Barzilai, A.; Confino, Y.; Schwartz, E. *J. Am. Acad. Dermatol.* **2003**, *49*, 672.
12. Sereno, D.; Alegre, A. M.; Silvestre, R.; Vergnes, B.; Ouaissi, A. *Antimicrob. Agents Chemother.* **2005**, *49*, 808.
13. MOE software package, version 03; Chemical computing groups Inc., Montreal, Canada.
14. SYBYL software package, version 6.9; Tripos Associates Inc.; 1699, S. Hanley Rd., St. Louis, MO 631444, USA.
15. Vergnes, B.; Sereno, D.; Madjidian-Sereno, N.; Lemesre, J. L.; Ouaissi, A. *Gene* **2002**, *296*, 139.
16. Vergnes, B.; Vanhille, L.; Ouaissi, A.; Sereno, D. *Acta Trop.* **2005**, *94*, 107.
17. Laskowski, R. A.; MacArthur, M. W.; Moss, A. *J. Appl. Crystallogr.* **1993**, *26*, 283.
18. Needleman, S. B.; Wunsch, C. D. *J. Mol. Biol.* **1970**, *48*, 443.
19. Avalos, J. L.; Bever, K. M.; Wolberger, C. *Mol. Cell* **2005**, *17*, 855.
20. Denu, J. M. *Trends Biochem. Sci.* **2003**, *28*, 41.
21. Sauve, A. A.; Celic, I.; Avalos, J.; Deng, H.; Boeke, J. D.; Schramm, V. L. *Biochemistry* **2001**, *40*, 15456.
22. Sauve, A. A.; Schramm, V. L. *Curr. Med. Chem.* **2004**, *11*, 807.
23. Sauve, A. A.; Schramm, V. L. *Biochemistry* **2003**, *42*, 9249.
24. Jackson, M. D.; Schmidt, M. T.; Oppenheimer, N. J.; Denu, J. M. *J. Biol. Chem.* **2003**, *278*, 50985.
25. Bhattacharrjee, A. K.; Karle, J. M. *Bioorg. Med. Chem.* **1998**, *6*, 1927.
26. Bhattacharrjee, A. K.; Karle, J. M. *Chem. Res. Toxicol.* **1999**, *12*, 422.